Contraction of the world's storm-cloud zones the primary contributor to the 21st century increase in the Earth's sunlight absorption

George Tselioudis

george.tselioudis@nasa.gov

NASA Goddard Institute for Space Studies

Jasmine Remillard

NASA/GISS https://orcid.org/0000-0003-3495-581X

Christian Jakob

ARC Centre of Excellence for the Weather of the 21st Century, Monash University

https://orcid.org/0000-0002-5012-3207

William Rossow

Franklin, NY

Physical Sciences - Article

Keywords:

Posted Date: September 20th, 2024

DOI: https://doi.org/10.21203/rs.3.rs-5050391/v1

Additional Declarations: There is **NO** Competing Interest.

Contraction of the world's storm-cloud zones the primary contributor to the 21st century increase in the Earth's sunlight absorption

George Tselioudis [(1)], Jasmine Remillard [(1)], Christian Jakob [(2)], and William B. Rossow [(3)]

(1) NASA/GISS, New York, NY, USA
(2) Monash University, Melbourne, Australia
(3) Franklin, NY, USA

Corresponding author:
George Tselioudis
NASA/GISS
2880 Broadway,
New York, NY 10026
USA
George.tselioudis@nasa.gov
gtselioudis@gmail.com

Abstract

Observations of the Earth's energy budget from the CERES instrument have shown that since the beginning of the 21st century the amount of sunlight absorbed by the Earth has been increasing at a rate of about 0.45 W/m^2 per decade, caused primarily by a decrease in sunlight reflection by clouds. This increase is a main component of the increase in the Earth's Energy Imbalance by about 0.5 W/m^2 between the first and second decades of the century. We analyze the CERES radiative budget trends of the past 23 years, with the objective to separate the contribution to those trends of changes in the large-scale atmospheric circulation and in local-scale cloud controlling processes. Regimes of large cloud cover and strong cloud radiative cooling are defined in the low latitude and the high latitude zones, representing the tropical rainy zone and the midlatitude storm zones respectively, and the trends in the areal coverage of those regimes over the past 23 years are examined along with the trends in the cloud solar radiative effect within each regime. This allows the decomposition of the global solar cloud radiative trends into circulation induced changes and those induced by local-scale processes. The results show that the circulation component of the cloud radiative changes, which manifests itself as a contraction of the midlatitude storm zones and the tropical rainy zone, is the dominant term in the solar reflection trend causing decreased sunlight reflection of 0.37 W/m^2 per decade. The discovery of this component provides a crucial missing piece in the puzzle of the 21st century increase of the Earth's Energy Imbalance and points to the large effect that even small atmospheric circulation changes have on the Earth's warming climate.

Introduction

Clouds modulate both the shortwave (SW) and longwave (LW) components of the Earth's energy budget and thus play a crucial role in determining the Earth's Energy Imbalance (EEI), which is defined as the difference between absorbed solar and emitted thermal radiation. The recent analyses of Clouds and the Earth's Radiant Energy System (CERES) data by Loeb et al. (2021, 2024) find that the past 20 years have experienced a significant increase of the EEI from about 0.5 W m^{-2} in the first decade to about 1 W/m^2 in the second one, and this is attributed primarily to an increase in the Absorbed SW Radiation (ASR) of 0.9 W/m^2 that is partially offset by an increase of 0.4 W/m^2 in the emitted thermal radiation. The increase in the absorbed solar radiation is driven primarily by a decrease in the reflection of SW radiation by clouds, that happens at a rate of 0.37 – 0.4 W/m^2 decade $^{-1}$ depending on the period analyzed. Loeb et al. (2024) find that large decreases in stratocumulus and mid-level clouds over the subtropics and decreases in low and mid-level clouds in the midlatitudes are the primary reason for the increasing absorbed SW trends in the northern hemisphere, while decreases in mid-level cloud reflection and a weaker reduction in low cloud reflection account for the increasing absorbed SW trend in the southern hemisphere. They point out that isolating the cloud contribution to the energy balance trends requires the removal of contributions from effective radiative forcing terms, such as aerosol-cloud indirect effects and greenhouse gas adjustments. Modeling studies using AMIP simulations (Raghuraman et al. 2021, Hodnebrog et al. 2024) suggest that the large ASR increases of the CERES period can only be explained as the additive contributions of effective radiative forcing and climate response to the warming, but the AMIP simulations end in 2014 thus limiting their usefulness in explaining the trends of the past two decades.

In a recent analysis of multiple satellite datasets, Tselioudis et al. (2024) examined the zonal mean trends of cloud and radiation properties during the satellite era. They found a poleward expansion of the subtropical small cloud cover region in both hemispheres along with a narrowing of the Intertropical Convergence Zone (ITCZ). Both these change patterns are likely connected to influences on the cloud field from the large-scale atmospheric circulation, whilst decreasing cloud cover trends within the subtropical cloud regime are more likely influenced by local cloud controlling processes. The observed cloud changes result in contrasting Shortwave Cloud Radiative Effect (SWCRE) changes between high and low latitude regions, with cloud radiative warming in the lower latitudes and near-zero changes or cooling in the higher ones.

In the present work, we analyze the 21st Century CERES radiative budget trends with the objective to separate the contribution to those trends of changes in large-scale atmospheric circulation and local-scale cloud controlling processes. Regimes of large cloud cover and strong SW cloud radiative cooling are defined in the low latitudes and the high latitude zones, representing the wet tropics associated with the ITCZ and the midlatitude storm tracks respectively. The trends in the areal coverage of the strong cloud radiative cooling regimes over the past 23 years are examined along with the trends in the

SW radiative effects of the clouds within each regime. This allows the decomposition of the global SWCRE trends into circulation induced changes in the areal coverage of the large and small cloud cover regimes and local-scale induced changes in the radiative properties of the clouds in each regime.

Datasets and Analysis

Starting in 2000 with the launch of the polar orbiting Terra satellite (and Aqua in 2002), the MODIS instruments provide cloud property data products (Platnick et al. 2021), while the CERES instruments flown on the same satellites measure top-of-atmosphere radiative fluxes (Loeb et al 2018). In the current analysis, the MODIS M3 Terra Total Cloud Cover (TCC) field is used to define the regimes of large TCC, while the CERES EBAF-Ed4.2 is used to derive the regimes of strong SWCRE. The SWCRE field is defined as the difference between the all-sky and the clear-sky SW fluxes.

The Large Total Cloud Cover (L-TCC) and Strong (large negative value) SWCRE (S-SWCRE) regimes are derived separately for the low latitudes (30^{o}S-30^{o}N) and the high latitude zones (30^{o}-90^{o} S/N) by identifying the maximum TCC and minimum SWCRE values at each zone in their respective climatologies, and then finding the locations of the maximum North-South gradient in TCC and SWCRE. The locations of maximum gradients are then connected to define the isoline thresholds that enclose the L-TCC and S-SWCRE regimes. Applying this method, in the low latitudes the L-TCC regime is defined as the area bounded by the 55% TCC isoline, and the regime of S-SWCRE as the area bounded by the -61W/m^2 isoline. In the high latitude zones, the L-TCC regime is defined as the area bounded by the 75% TCC isoline for both zones, and the S-SWCRE regime as the area bounded by the -65.5 W/m^2 isoline in the Southern and the -70 W/m^2 isoline in the Northern zone. Once the L-TCC and S-SWCRE regimes are defined, the area coverage of each regime and their trends are calculated for the 23-year period 2001-2023, along with the trends of the mean SWCRE values within and outside the S-SWCRE regime for the same period. This allows us to partition the global SWCRE trend into the contribution of the change of the S-SWCRE area coverage and the contribution of the change of the SWCRE values within the strong and weak SWCRE regimes, with the latter defined as all regions outside the strong SWCRE regime.

Results

Figure 1 shows the annual mean climatologies of the MODIS TCC (top) and the CERES SWCRE (bottom) fields, and with dotted lines the isoline boundaries of the L-TCC and the S-SWCRE regimes in the low and the high latitude zones. The plot shows that the L-TCC regimes delineate well the midlatitude storm tracks in the North Pacific, North Atlantic, and Southern Oceans, and the ITCZ and marine stratocumulus regions in the low latitudes. Roughly coincident regions of intense SW cloud cooling are apparent in the S-SWCRE plot,

with small differences between the two types of regimes occurring in the Arctic Ocean, the marine stratocumulus regions, and the coastline of the Antarctic. Those differences, with the TCC regime being generally more spatially extensive than the SWCRE one, come from the fact that the SW cloud radiative effect is not only affected by the cloud fraction, but also by the cloud optical depth and the reflectance of the underlying surface.

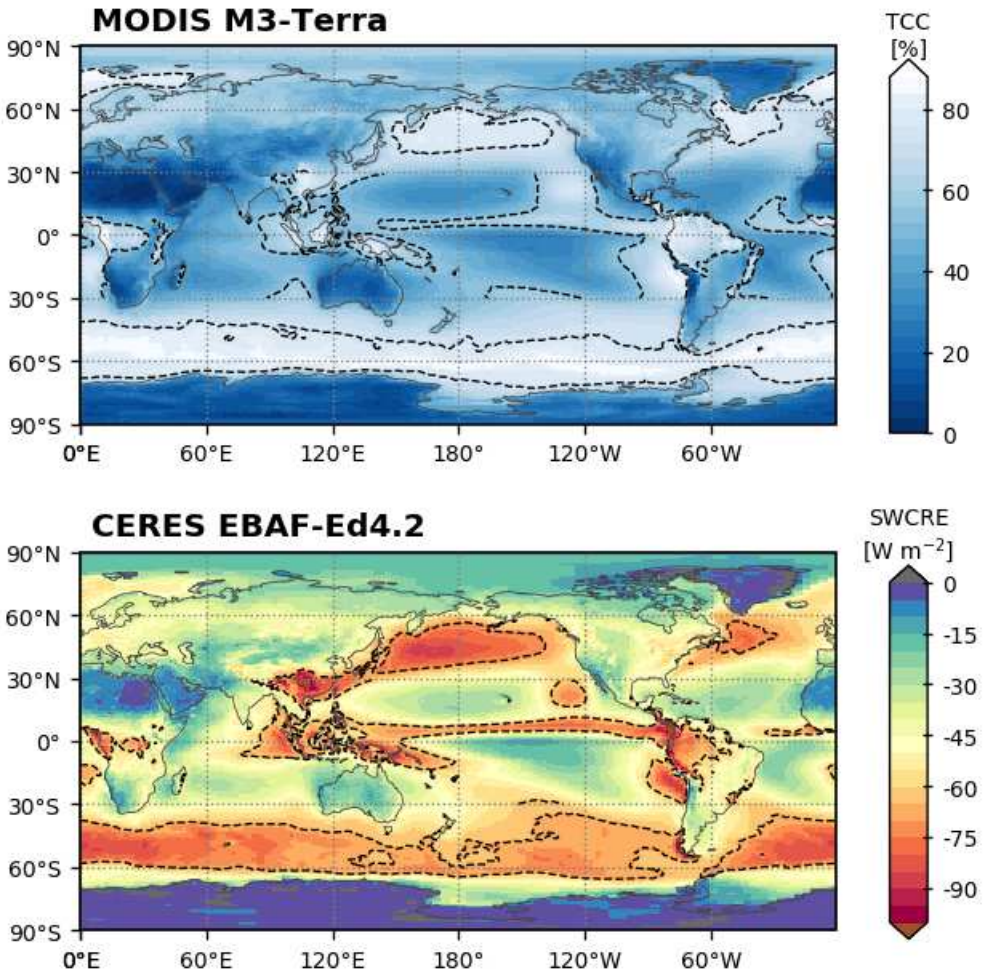

Figure 1: *Annual mean maps of MODIS TCC (top) and the CERES SWCRE (bottom) for the 2001-2023 period. Dotted lines indicate the isoline boundaries of the L-TCC and the S-SWCRE regimes as defined in the text.*

The time trends of the annual mean percent area coverage of the L-TCC (top) and the S-SWCRE (bottom) regimes for the 2001-2023 period are shown in Figure 2, for the low latitude and the two high latitude zones. In all three climate zones, the area coverage of the L-TCC region shows statistically significant decreases that range from 1.59% to 2.88% per decade, indicating a contraction of the midlatitude storm regions and a narrowing of the

ITCZ region, trends that were also found in Tselioudis et al. (2024). In the present analysis, the tropical downward L-TCC trend may also be due to a contraction of the marine stratocumulus regions, but such a contraction was not observed in the zonal mean analysis of Tselioudis et al. (2024). Also, the Southern high latitude L-TCC area time series has an unusually low value in 2021, but removal of that year changes very little the slope of the trend and does not affect the trend significance. In accordance with the L-TCC area coverage trends, the area coverage of the S-SWCRE regimes shows significant decreasing trends in all climate zones, with slopes that range from 0.88% to 1.32% per decade, implying a significant global-scale decrease in the area coverage of the regimes of strong cloud radiative cooling.

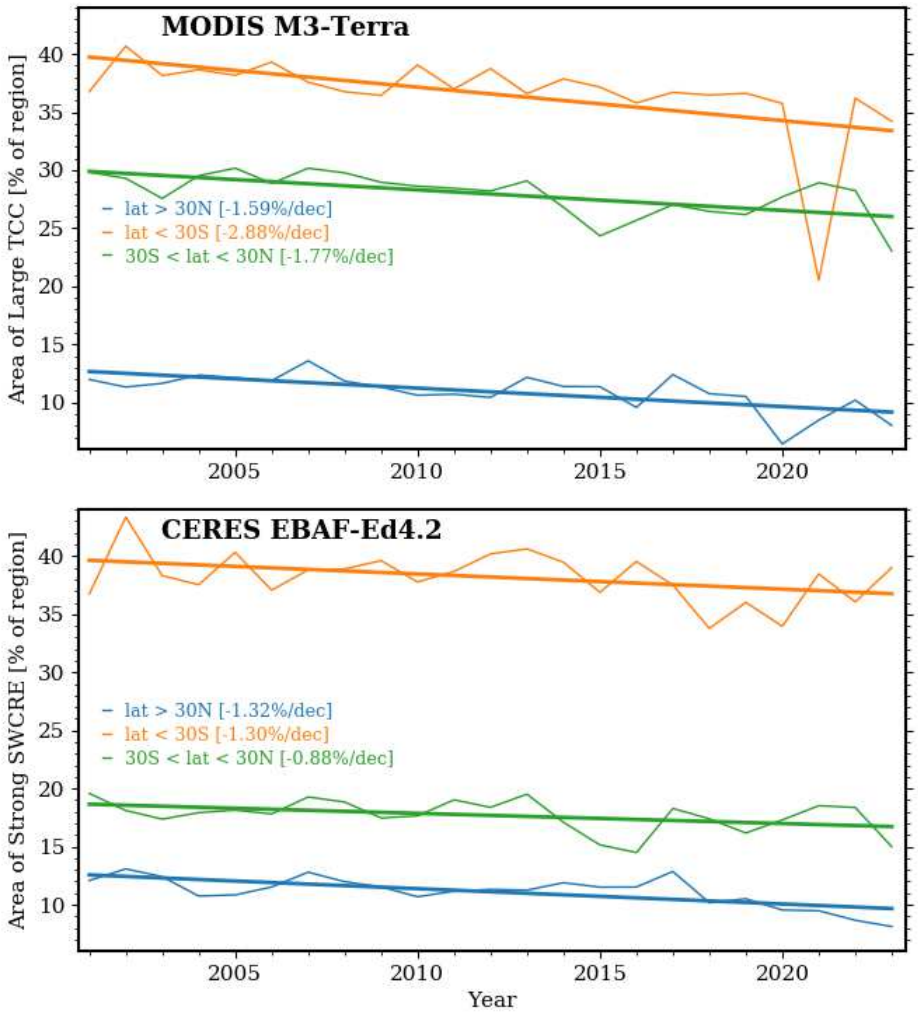

Figure 2: *Time series of the annual mean percent area coverage of the L-TCC (top) and S-SWCRE (bottom) regimes for the 2001-2023 period, for the two high latitude and the low latitude zones. Lines depict linear regressions and solid lines indicate trends significant at the 95% level.*

The analysis of Loeb et al. (2024) finds an increasing global trend in SWCRE of 0.37 W/m^2 per decade for the 3/2000-12/2022 period, and this trend is the largest component of the increasing trend in absorbed SW radiation. Figure 3 shows the CERES annual trends in SWCRE for the globe, the low and the high latitude zones for the 2001-2023 period. The global trend for that period is 0.45 W/m^2 per decade, and the trend for all climate zones is positive, with SWCRE increasing (or cloud radiative cooling decreasing) by 0.44 W/m^2/decade in the Northern and 0.25 W/m^2/decade in the Southern high latitudes, and by 0.56 W/m^2/decade in the low latitudes. Since in the same period the area coverage of the S-SWCRE regimes in all climate zones is decreasing (Fig. 2-bottom), next we will quantify the contribution of this regime area contraction to the SWCRE trends. Note that the L-TCC regime area trends (Fig. 2-top) do not enter the calculation of the decomposed SWCRE trends.

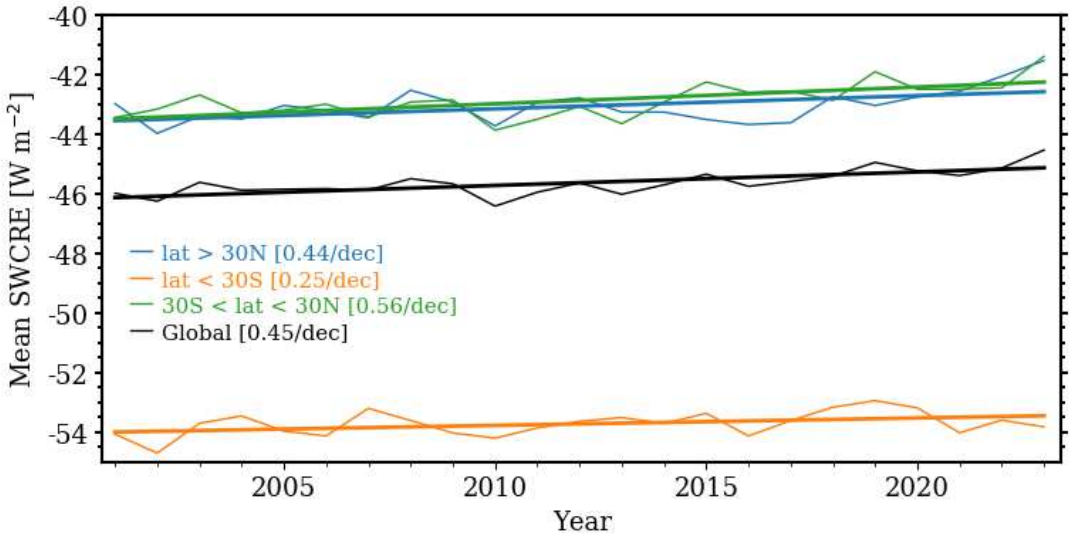

Figure 3: *Time series of CERES annual mean SWCRE values for the globe, low latitude, and high latitude zones for the 2001-2023 period. Lines depict linear regressions and solid lines indicate trends significant at the 95% level.*

Following Williams and Tselioudis (2007), the average SW cloud radiative effect over a climate zone $\overline{\text{SWCRE}}$ can be derived from the Strong- and Weak-SWCRE regimes as:

$$\overline{\text{SWCRE}} = \alpha\overline{\text{S-SWCRE}} + (1-\alpha)\overline{\text{W-SWCRE}} \quad (1)$$

Where α is the percent area coverage of the S-SWCRE regime. Then, the trends in $\overline{\text{SWCRE}}$ can be decomposed into the contributions of the change in area coverage and in the mean properties of the Strong- and Weak-SWCRE regimes as follows:

$$\Delta\overline{\text{SWCRE}} = \overline{\text{S-SWCRE}}\,\Delta\alpha + \overline{\text{W-SWCRE}}\,(1-\Delta\alpha) + \alpha\,\Delta\overline{\text{S-SWCRE}} + (1-\alpha)\,\Delta\overline{\text{W-SWCRE}} + \Delta\overline{\text{S-SWCRE}}\,\Delta\alpha + \Delta\overline{\text{W-SWCRE}}\,(1-\Delta\alpha) \quad (2)$$

Since the last two covariance terms of Eq. 2 are small, Table 1 summarizes the first four terms of the equation for the three climate zones. The first two terms represent the part of the SWCRE trend coming from the change in the area coverage of the S-SWCRE regime and the corresponding opposing change in the area of the W-SWCRE regime, and the third and fourth terms represent the part of the SWCRE trend coming from changes in the mean SWCRE values within the S-SWCRE and the W-SWCRE regimes. In all climate zones, the dominant trend is the SW cloud radiative warming is coming from the contraction of the S-SWCRE regimes and the corresponding expansion of the W-SWCRE regimes. In the high latitude zones, the contraction of the S-SWCRE midlatitude storm regions and the corresponding expansion of the W-SWCRE regions produce an additive cloud radiative warming of 0.51 W/m^2/decade in the Northern and 0.37 W/m^2/decade in the Southern zone. This is partially counteracted by an increase in cloud radiative cooling within the W-SWCRE regime of 0.13 W/m^2/decade in the Northern and 0.27 W/m^2/decade in the Southern zone and is aided by a small cloud radiative warming within the S-SWCRE regime of 0.06 W/m^2/decade in the Northern and 0.12 W/m^2/decade in the Southern region. In the low latitudes, the contraction of the S-SWCRE ITCZ region and the corresponding expansion of the of the W-SWCRE region produce an additive cloud radiative warming of 0.3 W/m^2/decade, which is aided by a cloud radiative warming within the W-SWCRE regime of 0.28 W/m^2/decade.

SWCRE Trend Components (W/m^2/decade)	N-HiLat	S-HiLat	LoLat
$\overline{\text{S-SWCRE}}\ \Delta\alpha$	1.02	0.93	0.62
$\overline{\text{W-SWCRE}}\ (1-\Delta\alpha)$	-0.51	-0.55	-0.32
$\alpha\ \Delta\overline{\text{S-SWCRE}}$	0.06	0.12	-0.02
$(1-\alpha)\ \Delta\overline{\text{W-SWCRE}}$	-0.13	-0.27	0.28

Table 1: *First four terms of Equation 2 (as defined in the text) for the two high latitude and the tropical zones.*

The decomposition of the SWCRE trend can be further simplified if we conjecture that the contraction of the areal coverage of the S-SWCRE storm track and ITCZ regions, and the corresponding expansion of the W-SWCRE regimes, constitute the large-scale circulation components of the trend, while the changes in the mean SWCRE values within the S-SWCRE and W-SWCRE regimes constitute the local-scale cloud controlling processes

components of the trend. Furthermore, the Northern and Southern high latitude zones exhibit SWCRE component trends that are identical in sign and very close in magnitude and thus their trends can be merged into one high latitude zone result. Following those simplifications, Figure 4 and Table 2 show the large-scale circulation and local-scale process components of the SWCRE trends for the high latitude regions, the low latitude region, and the globe. The local-scale process component is broken into the S-SWCRE and W-SWCRE parts, since the two parts exhibit different signs and magnitudes (Table 1).

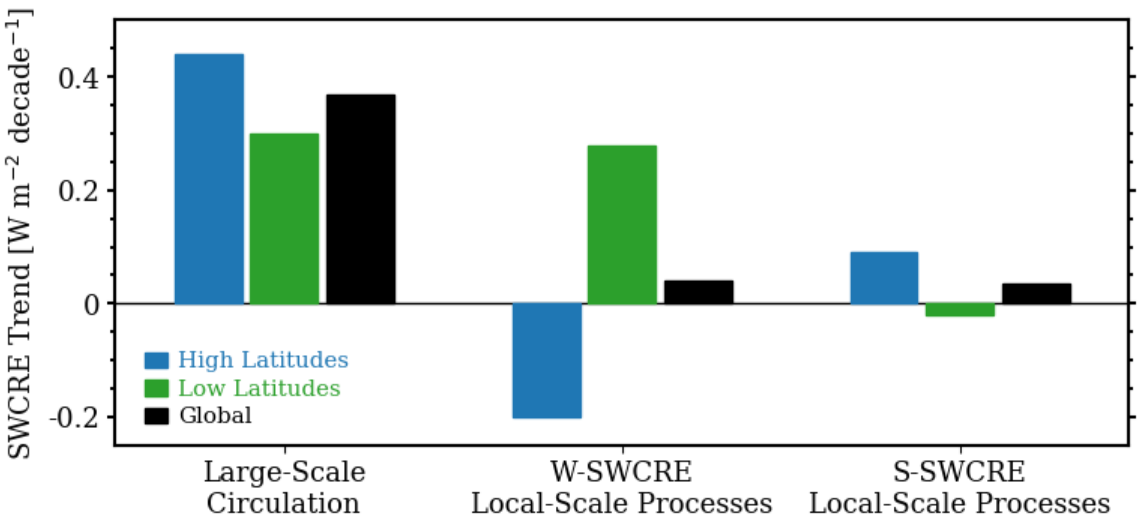

Figure 4: *Large-scale Circulation and Small-scale Process components of the SWCRE trends as defined in the text, for the high-latitude regions, the low-latitude region, and the globe.*

SWCRE Trend Components (W/m^2/decade)	HiL	LoL	GL
LARGE-SCALE CIRCULATION COMPONENT	0.44	0.3	0.37
S-SWCRE LOCAL-SCALE PROCESSES COMPONENT	0.09	-0.02	0.035
W-SWCRE	-0.2	0.28	0.04

Table 2: *Large-scale Circulation and Small-scale Process components of the SWCRE trends as defined in the text, for the high-latitude regions, the low-latitude region, and the globe.*

The results on Figure 4 and Table 2 show that the increasing global mean SWCRE trend of 0.45 W/m^2/decade comes predominately from the large-scale circulation component, which is driven primarily by a high latitude cloud radiative warming of 0.44 W/m^2/decade resulting from the contraction of the midlatitude storm regimes and a tropical cloud radiative warming of 0.3 W/m^2/decade resulting from the narrowing of the ITCZ region. The local-scale processes component contributes a low latitude cloud radiative warming trend of 0.28 W/m^2/decade in the W-SWCRE regime which is counteracted by a cloud radiative cooling trend of 0.2 W/m^2/decade in the W-SWCRE regimes of the high latitude zones, while the trends in this component for the S-SWCRE regimes of the two climate zones are small and of opposite sign. As a result, of the 0.45 W/m^2/decade global SW cloud radiative warming trend, 0.37 W/m^2 are due to the contraction of the world's midlatitude storm and tropical convergence zones.

Discussion

Our results show that global SWCRE trends are predominantly caused by changes in large-scale circulation features and are the result of areal coverage changes of the S-SWCRE and W-SWCRE regions, which have a very large difference in the mean SWCRE values between them. In the high latitude zones this difference is around 38 W/m^2 and 30 W/m^2 in the Northern and Southern zones respectively, and therefore a reduction of about 1.3% per decade in the S-SWCRE regime area coverage and its replacement by the W-SWCRE regime produces SW cloud radiative warming of 0.5 W/m^2/decade and 0.37 W/m^2/decade respectively. In the low latitudes, the difference in mean values between the two SWCRE regimes is 34 W/m^2, and the 0.87% decrease of the area coverage of the S-SWCRE regime and its replacement by the W-SWCRE regime produces cloud radiative warming of 0.3 W/m^2/decade. The within-regime local-scale process SWCRE trend components are only significant in the W-SWCRE regime and, even though in the low latitudes the local-scale process component is of similar magnitude to the large-scale circulation one, the tropical and high latitude local-scale components are of opposite sign and that contrast further increases the dominance of the circulation component in the global SWCRE trend.

The large-scale circulation component of the recent SWCRE trends consist of a contraction of the midlatitude storm cloud zone and a narrowing of the ITCZ zone, both changes that have also been documented in Tselioudis et al. (2024). The midlatitude storm cloud contraction is indicative of effects on the cloud field by a widening of the Hadley circulation and a poleward shift in the midlatitude storm tracks, both trends that have been documented in recent studies (e.g. Grise et al. 2018, Staten et al. 2020, Woollings et al. 2023). The narrowing of the ITCZ has also been documented in precipitation-based observational analysis and in modeling studies (Wodzicki and Rapp 2016, Byrne et al. 2018), and explanations have been proposed based on energetic and potential dynamical theories (Byrne et al. 2018). The narrowing and strengthening of the ITCZ can also be seen as a forcing of the Hadley cell widening, through additional latent heat release (e.g. Rind and Rossow 1984) and the balancing of this heat release through extension of the radiative

cooling subsidence zone to maintain Radiative Convective Equilibrium (Jakob et al. 2019). The local-scale process component of the SWCRE trends is significant in the W-SWCRE regimes and consist of contrasting cloud radiative cooling trends in the high latitude zones and cloud radiative warming trend in the low latitudes. This contrast can be caused by high latitude low-cloud albedo increases due to the 'cloud phase feedback' (e.g. Tan et al. 2016, Fey and Kay 2017), and low latitude low-cloud fraction decreases due to boundary layer processes or aerosol indirect effects (Webb et al. 2024, Hodneborg et al. 2024). The latitudinal contrast in the SWCRE trends is also documented for the satellite era in Tselioudis et al. (2024).

The present study shows that, due to the contraction of the world's storm cloud zones, the large-scale circulation component constitutes the dominant term of the recent increases in absorbed solar radiation and provides a crucial missing piece in the puzzle of the 21st century increase of the Earth's Energy Imbalance and the large heat anomaly of 2023 (Schmidt 2024). The large SWCRE differences between the large-scale circulation regimes defined in this work, implies that changes of only a few percent in the relative coverage of the regimes produce large cloud radiative signatures that can dominate the radiative balance trends, and this makes it imperative to understand and simulate correctly the future evolution of the current trend of storm-cloud area contraction.

Funding

This work was supported by the NASA Modeling, Analysis, and Prediction (MAP) program.

Data availability

The present work has not produced any original data. The datasets used in the analysis are all specified in the text and in the references.

References

Byrne, M. P., A. G. Pendergrass, A. D. Rapp, and K. Wodzicki, 2018: Response of the Intertropical Convergence Zone to climate change: Location, width, and strength. Curr. Clim. Change Rep., 4, 355-370, doi:10.1007/s40641-018-0110-5.

Frey, W. R., & Kay, J. E., 2017: The influence of extratropical cloud phase and amount feedbacks on climate sensitivity. Climate Dynamics, 50, 3097–3116.

Grise, K. M., and Coauthors, 2019: Recent tropical expansion: Natural variability or forced response? J. Climate, 32, 1551–1571, https://doi.org/10.1175/JCLI-D-18-0444.1.

Hodnebrog Ø, Myhre G, Jouan C, Andrews T, Forster PM, Jia H, Loeb NG, Olivié DJL, Paynter D, Quaas J, Raghuraman SP, Schulz M (2024) Recent reductions in aerosol emissions have increased Earth's energy imbalance. Nature Comm Earth Environ. https://doi.org/10.1038/s43247-024-01324-8

Jakob, C., Singh, M. S., & Jungandreas, L. (2019). Radiative convective equilibrium and organized convection: An observational perspective. Journal of Geophysical Research: Atmospheres, 124, 5418–5430. https://doi.org/10.1029/2018JD030092

Loeb, N.G., Ham, SH., Allan, R.P. et al. Observational Assessment of Changes in Earth's Energy Imbalance Since 2000. Surv Geophys (2024). https://doi.org/10.1007/s10712-024-09838-8

Loeb NG, Johnson GC, Thorsen, TJ *et al.,* 2021: Satellite and ocean data reveal marked increase in Earth's heating rate. *Geophys Res Lett*; **48**:e2021GL093047

Loeb, N.G.; Doelling, D.R.; Wang, H.; Su, W.; Nguyen, C.; Corbett, J.G.; Liang, L.; Mitrescu, C.; Rose, F.G.; Kato, S., 2018: Clouds and the Earth's Radiant Energy System (CERES) Energy Balanced and Filled (EBAF) Top-of-Atmosphere (TOA) Edition-4.0 Data Product. J. Clim., 31, 895–918.

Platnick S, Meyer K, Wind G, Holz RE, Amarasinghe N, Hubanks PA, Marchant B, Dutcher S, Veglio P., 2021: The NASA MODIS-VIIRS Continuity Cloud Optical Properties Products. Remote Sensing. 13(1):2. https://doi.org/10.3390/rs13010002

Raghuraman SP, Paynter D, Menzel R, Ramaswamy V (2023) Forcing, cloud feedbacks, cloud masking, and internal variability in the cloud radiative effect satellite record. J Clim 36:4151–4167. https://doi.org/10.1175/JCLI-D-22-0555.1

Rind, D., and W.B. Rossow, 1984: The effects of physical processes on the Hadley circulation. J. Atmos. Sci., 41, 479-507, doi:10.1175/1520-0469(1984)041<0479:teoppo>2.0.co;2.

Schmidt, G.A., 2024: Climate models can't explain 2023's huge heat anomaly — We could be in uncharted territory. Nature, 627, 467, doi:10.1038/d41586-024-00816-z.

Staten, P. W., and Coauthors, 2020: Tropical Widening: From Global Variations to Regional Impacts. Bull. Amer. Meteor. Soc., 101, E897–E904, https://doi.org/10.1175/BAMS-D-19-0047.1.

Tan, I., Storelvmo, T., & Zelinka, M. D., 2016: Observational constraints on mixed-phase clouds imply higher climate sensitivity. Science, 352, 224–227.

Tselioudis, G., W.B. Rossow, F. Bender, L. Oreopoulos, and J. Rémillard, 2024: Oceanic cloud trends during the satellite era and their radiative signatures. Clim. Dyn., early online, doi:10.1007/s00382-024-07396-8.

Webb, M. J., Lock, A. P., & Ogura,T., 2024: What are the main causes of positive subtropical low cloud feedbacks in climate models? Journal of Advances in Modeling Earth Systems, 16, e2023MS003716. https://doi.org/10.1029/2023MS003716

Williams, K.D., and G. Tselioudis, 2007: GCM intercomparison of global cloud regimes: Present-day evaluation and climate change response. Clim. Dyn., 29, 231-250, doi:10.1007/s00382-007-0232-2.

Wodzicki, K. R., and A. D. Rapp, 2016: Long-term characterization of the Pacific ITCZ using TRMM, GPCP, and ERA-Interim, *J. Geophys. Res. Atmos.*, 121, 3153–3170, doi:10.1002/2015JD024458.

Woollings, T., Drouard, M., O'Reilly, C.H. et al., 2023: Trends in the atmospheric jet streams are emerging in observations and could be linked to tropical warming. Commun Earth Environ 4, 125. https://doi.org/10.1038/s43247-023-00792-8